Physics – Uspekhi **61** (2) 191 – 202 (2018)

PHYSICS OF OUR DAYS

PACS numbers: 91.25.Cw, 91.25.Mf, 94.20.wq

1000th issue of *Uspekhi Fizicheskikh Nauk* journal

What humankind can expect with an inversion of Earth's magnetic field: threats real and imagined

O O Tsareva, L M Zelenyi, H V Malova, M V Podzolko, E P Popova, V Yu Popov

DOI: https://doi.org/10.3367/UFNe.2017.07.038190

Contents

Abstract. Earth's global magnetic field generated by an internal dynamo mechanism has been continuously changing on different time scales since its formation. Paleodata indicate that relatively long periods of evolutionary changes can be replaced by quick magnetic inversions. Based on observations, Earth's magnetic field is currently weakening and the magnetic poles are shifting, possibly indicating the beginning of the inversion process. This paper invokes Gauss coefficients to approximate the behavior of Earth's magnetic field components over the past 100 years. Using the extrapolation method, it is estimated that the magnetic dipole component will vanish by the year 3600 and at that time the geomagnetic field will be determined by a smaller value of a quadrupole magnetic component. A numerical model is constructed which allows evaluating and comparing both galactic and solar cosmic ray fluxes in Earth's magnetosphere and on its surface during periods of dipole or quadrupole domination. The role of the atmosphere in absorbing particles of cosmic rays is taken into account. An estimate of the radiation danger to humans is obtained for the ground level and for the International Space Station altitude of $\sim$ 400 km. It is shown that in the most unfavorable, minimum field interval of the inversion process, the galactic cosmic ray flux increases by no more than a factor of three, implying that the radiation danger does not exceed the maximum permissible dose. Thus, the danger of magnetic inversion periods generally should not have fatal consequences for humans and nature as a whole, despite dramatically changing the structure of Earth's magnetosphere.

Keywords: geomagnetic dynamo, magnetic field inversion, geomagnetic field, modeling, galactic cosmic rays, solar cosmic rays, radiation safety

O O Tsareva Space Research Institute, Russian Academy of Sciences, ul. Profsoyuznaya 83/32, 117997 Moscow, Russian Federation
E-mail: olga8.92@mail.ru
L M Zelenyi Space Research Institute, Russian Academy of Sciences, ul. Profsoyuznaya 83/32, 117997 Moscow, Russian Federation; Moscow Institute of Physics and Technology (State University), Institutskii per. 9, 141700 Dolgoprudnyi, Moscow region, Russian Federation
E-mail: lzelenyi@iki.rssi.ru
H V Malova Lomonosov Moscow State University, Skobeltsyn Institute of Nuclear Physics, Leninskie gory 1, str. 2, 119991 Moscow, Russian Federation; Space Research Institute, Russian Academy of Sciences, ul. Profsoyuznaya 83/32, 117997 Moscow, Russian Federation
E-mail: hmalova@yandex.ru
M V Podzolko Lomonosov Moscow State University, Skobeltsyn Institute of Nuclear Physics, Leninskie gory 1, str. 2, 119991 Moscow, Russian Federation
E-mail: spacerad@mail.ru
E P Popova Lomonosov Moscow State University, Skobeltsyn Institute of Nuclear Physics, Leninskie gory 1, str. 2, 119991 Moscow, Russian Federation; Schmidt Institute of Physics of the Earth, Russian Academy of Sciences, ul. B. Gruzinskaya 10, str. 1, 123242 Moscow, Russian Federation
E-mail: popovaelp@mail.ru
V Yu Popov National Research University 'Higher School of Economics', ul. Myasnitskaya 20, 101000 Moscow, Russian Federation; Lomonosov Moscow State University, Faculty of Physics, Leninskie gory 1, str. 2, 119991 Moscow, Russian Federation
E-mail: E-mail: masterlu@mail.ru

Received 27 June 2017, revised 27 July 2017
Uspekhi Fizicheskikh Nauk **188** (2) 207 – 220 (2018)
DOI: https://doi.org/10.3367/UFNr.2017.07.038190
Translated by K A Postnov; edited by A Radzig

1. Introduction

Earth's magnetic field undergoes cyclic variations on different timescales ranging from minutes, days, and hundreds of years up to several million years. The longest global changes in the geomagnetic field — inversions — represent reversals of the magnetic field direction, which very crudely can be considered a magnetic dipole field. Paleomagnetic data based on the thermoremanent magnetization of massive materials suggest that the inversions have happened several

times over Earth's geological history [1–3]. The restored history of the geomagnetic field inversions (magnetochronological scale) spans a period of about four bln years. The present magnetic epoch (the period between magnetic polarity changes), which is known as the Brunhes epoch, started about 730 thousand years ago, after the Matuyama epoch [2, 4–6]. Detailed research has established that short periods of polarity changes, so-called episodes, occurred inside the epochs. For example, during the Matuyama epoch, the Jaramillo episode is known to have happened about one million years ago, in which the inverse magnetic field lasted for about 60 thousand years, a relatively short time interval. According to estimates, the inversion itself can last from 100 years (with a dipole inclination decay of about 2° per year according to Ref. [7]) up to approximately 5–10 thousand years [8–10].

As a rule, the magnetic field inversions occur against the background of a significant weakening of the geomagnetic field, which started before the polarity changes. Prior to the polarity change, the amplitude of secular variations increases [5, 11]. The motion of the virtual magnetic pole (the line connecting the North and South Magnetic Poles) during the inversions is rather chaotic but occurs within a limited longitude band. During the inversions, Earth's magnetic field (also called paleomagnetic) is most likely multipole and can be described by models based on the geomagnetic dynamo mechanism [4, 12–14]. In several papers, magnetic field models are used to reconstruct the structure of the magnetosphere during the geomagnetic field inversions and to assess their impact on the circumterrestrial space (for example, using magneto-hydrodynamic (MHD) models as presented in papers [10, 15–17]). It should be noted, however, that the effect of the geomagnetic field inversions on the global structure of the magnetosphere, on the system of electric currents in it and on the magnetospheric plasma content is far from fully understood.

The magnetic inversions are thought to occur chaotically [4]. The periods between them can last from several dozen thousand years to several million years. The last field reversal occurred about 730 thousand years ago at the border between the Matuyama and Brunhes epochs [18]. That a new magnetic field inversion is possibly starting now can be inferred from magnetic field changes over the last hundred years, shown in Fig. 1. This figure is constructed using the IGRF (International Geomagnetic Reference Field) model of Earth's magnetic field in the period from 1900 until 2020. The figure suggests that a significant shift in the location of the magnetic poles (the points on the conventional surface of Earth at which the magnetic field is strictly normal to the surface) is occurring during this period: the North and South Poles have shifted by more than 2000 km and 1000 km, respectively. Here, the change in the location of the 'geomagnetic' poles of the central and shifted dipoles [19] (the points at which the dipole axis crosses Earth's surface) is not very large. At the same time, the magnetic dipole moment has decreased by 7.5%, while the contribution from the high-order harmonics of the magnetic field, in contrast, has increased by $\sim 50\%$. In the preceding several centuries, the rate of the weakening of the dipole field was 5% per century [20]. These data enable us to suggest that the inversion process will not appear to be a literally 'dipole overturn', but a transformation of the dipole into a multipole (and eventually the formation of a new dipole with the opposite location of the poles).

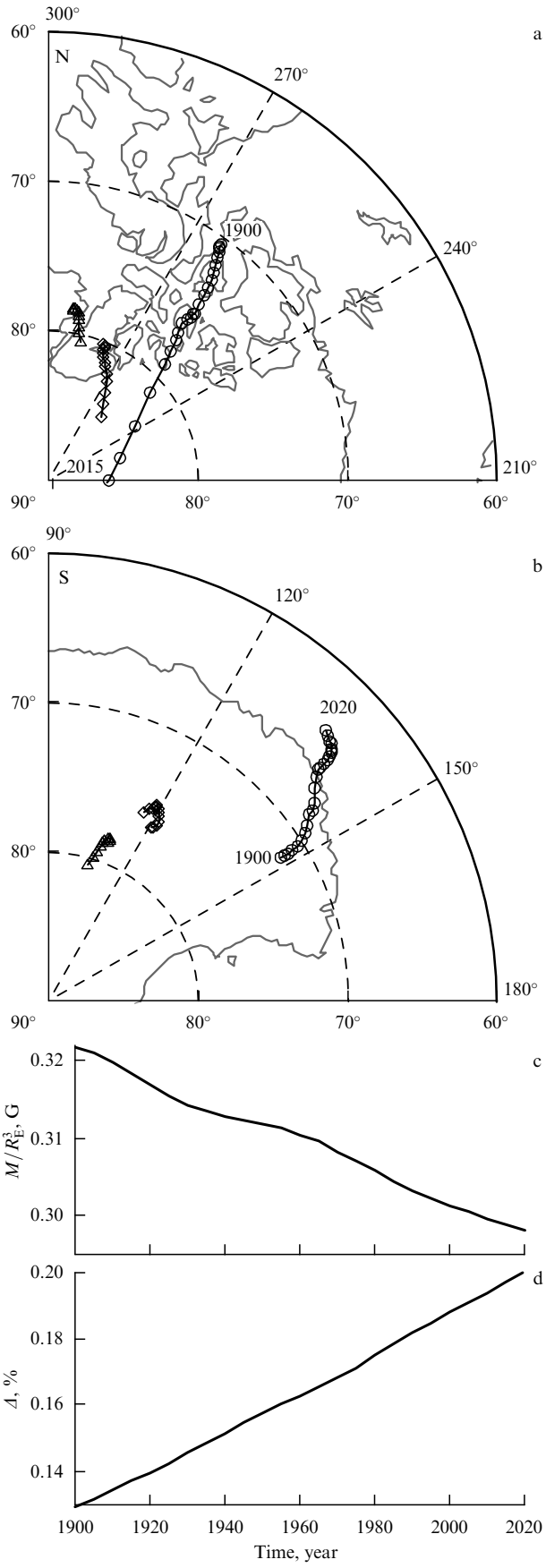

Figure 1. Changes in the locations of (a) North and (b) South Magnetic Poles (circles) and geomagnetic (triangles — dipole, diamonds — shifted dipole) poles; (c) the magnetic dipole moment M, and (d) the contribution Δ of the 2nd and 3rd magnetic field harmonics from 1900 until 2020.

An important factor affecting the formation of the upper atmosphere and ionosphere of Earth and undoubtedly impacting the biosphere is the incoming flux of galactic cosmic rays (GCRs) — atomic nuclei accelerated to energies from 10^9 to 10^{20} eV. GCRs consist of 90% protons, 7% alpha-particles, and 3% charged nuclei with $Z > 2$ and electrons. In the whole, Earth's magnetic field deflects charged particles; therefore, only particles with energies exceeding some threshold value can enter the atmosphere. For example, at a latitude of 50° north, the magnetic cut-off (the threshold energy of particles) is 0.66 GeV for protons, and 1.3 GeV for alpha-particles. The magnetic cut-off value depends on the latitude: it is higher at the equator than near the magnetic poles. Charged particles with energies below the threshold ones are mostly captured by the magnetosphere and are distributed inside it by filling the magnetospheric structures: Van Allen belts, the plasma sheet of the tail, the ring current, etc.

At altitudes on the order of several dozen kilometers from the ground, primary cosmic rays strongly interact with atomic nuclei of the air to produce pions (π), kaons (K), nucleon–antinucleon pairs, hyperons, and other elementary particles. The charged pions ($\pi^{\pm}$) produced either decay to form muons and neutrinos or further interact with nuclei. At ultrahigh energies of the primary particles ($E > 10^5$ GeV), the number of secondary progeny particles that form so-called extensive air showers (EASs) in nuclear and electron–photon cascades in Earth's atmosphere becomes as high as $10^6 - 10^9$. Thus, the impinging of GCRs into the atmosphere can initiate the development of cascades of nuclear active particles, as well as electron–photon cascades. The maximum muon generation occurs at altitudes of $\sim 10-20$ km. Fluxes of high-energy muons are weakly absorbed in the atmosphere; therefore, secondary cosmic radiation at sea level mostly consists of muons (the hard component with an intensity of $J_\mu = 0.82 \times 10^{-2}$ cm^{-2} s^{-1} sr^{-1}), electrons, and photons (the soft component with an intensity of $J_\nu = 0.31 \times 10^{-2}$ cm^{-2} s^{-1} sr^{-1}).

The spatial distribution of these fluxes in the terrestrial magnetosphere depends on the geomagnetic field configuration, and their value is determined by solar activity and the perturbed state of the geomagnetic field. The GCR intensity is established to change by a factor of two in counterphase with the solar activity. This is due to the fact that during periods of maximum solar activity, the perturbed heliospheric magnetic field deflects charged particles incoming from deep space. During the solar activity minimum, the cosmic radiation intensity is about $J \sim 0.2$ cm^{-2} s^{-1} sr^{-1}, and during the solar maximum, it is $J \sim 0.08$ cm^{-2} s^{-1} sr^{-1}. Nuclear interactions of the GCR particles with atmospheric atoms ultimately change its composition and density. The atmosphere characteristics also change due to precipitation of particles captured in the Van Allen radiation belts. Thus, to analyze and forecast the atmospheric state, the spatial distribution and energy spectra of GCR particle fluxes should be known. To do this, numerical models have been elaborated that take into account the change in charged particle fluxes, depending on the solar activity. Such models should be used jointly with the model of charged particle penetration into Earth's magnetosphere.

The terrestrial magnetosphere is a target not only for GCRs, but also for solar cosmic rays (SCRs), which are accelerated charged particles ejected from the Sun by solar flares or during decays of prominences. The ejected particles (protons, electrons, and light nuclei with an energy from 0.1 MeV to several hundred MeV and even several dozen GeV) can reach Earth's orbit after interacting with the interplanetary medium. The effect of SCR on Earth's magnetosphere mainly appears either at high altitudes [for example, in the orbit of the International Space Station (ISS)] or indirectly through filling of the Van Allen belts, magnetospheric storms, polar precipitations of particles, etc. The intruding SCRs into the ionosphere at polar latitudes can lead to additional ionization and corresponding worsening of short-wavelength radio communications. There is evidence that SCRs can significantly damage the terrestrial ozone layer. Enhanced fluxes of SCRs can also be important sources of radiation hazard for astronauts and equipment on board space vehicles. As for the radiation hazard on Earth, most SCRs, being less energetic than GCRs, are cutoff by Earth's magnetic field and are absorbed in the atmosphere; therefore, SCRs cannot significantly affect the terrestrial radiation background.

A detailed picture of magnetic field behavior during inversions is absent because of the complexity of analysis of paleomagnetic data and the long timescales of these events [20, 21]. The geomagnetic field is known to have a quadrupole component, in addition to the dipole one, as well as higher-order multipoles. There is some evidence that the total energy of the magnetic field does not vary significantly during inversions, i.e., part of the energy of the dipole magnetic field can be redistributed among higher-order multipole moments [22–24]. However, the amplitudes of these components rapidly decrease with distance, and in the case of diminishing of the dipole component during inversion, the quadrupole component will become dominant. Some data (see, for example, Ref. [23]) suggest that during certain inversions with dipole decay, the quadrupole component could dominate and its amplitude increase by about 10% compared to the present-day level. Such was a possible magnetic field configuration during the Jaramillo inversion [25].

The magnetic field evolution during inversion can be calculated using dynamo models [4]. As there is no clear understanding of the flow of matter in Earth's interior, the dynamo models can reproduce different scenarios of the magnetic field evolution during the inversions, depending on the assumed behavior of matter in the liquid core of Earth. Estimates show that the diminishing of the geomagnetic field during inversion results in an increased GCR flux in the inner magnetosphere and an enhanced GCR/SCR flux intensity near Earth, in particular at altitudes of the trajectories of space satellites and the ISS. Inversion is a relatively rare event that has never occurred during the era of *homo sapiens* on Earth, so its inevitable advent clearly causes some trouble and poses the question of the radiation hazard for humans during the inversion. The issues of the cosmic radiation hazard for the bio- and technosphere, the 'blow-off' of Earth's atmosphere to outer space, ozone layer disappearance and other elements of a possible ecological catastrophe, which are frequently discussed in the literature and by the mass media, are beyond the scope of the present paper.

In this paper, we study the flux levels of GCR/SCR protons and the radiation safety on Earth and in the circumterrestrial space during magnetic inversion using the most realistic scenario (a decrease in the magnetic dipole field by 10% or to zero during the inversion). To justify the

inversion regime, we construct a geomagnetic dynamo model to estimate the general trend in the changes of the geomagnetic field multipolar components. Based on extrapolation of the field decomposition coefficients, we estimate when the inversion will begin, the dipole field will vanish, and later the sign of the magnetic field will change across Earth's entire surface. Using a numerical model of Earth's magnetosphere during the inversion and by integrating trajectories of GCR/SCR particles, we estimate radiation doses at altitudes of 400 and 100 km, as well as on the ground level. We also estimate the regions of precipitation of energetic particles onto Earth's surface.

2. Geomagnetic dynamo model

To study geomagnetic field inversion regimes, we have used a nonlinear $\alpha\Omega$-dynamo model described in Ref. [26] [see equations (1), (2)], taking into account that the radius restricting the outer liquid core of Earth, where the magnetic field generation takes place, is about 1/3 of the planet's radius. We have analyzed the parametric space for the dipole and quadrupole field proceeding from the low-mode approximation [27].

It should be noted that the low-mode approximation is one of the possible means of obtaining simplified models to clarify the physics of the magnetic field generation in celestial bodies. It is assumed that the excited magnetic field of a star or a planet can be described by a comparatively small number of parameters, which enables one to substitute the dynamo equations with a suitably chosen dynamical system of equations of not-too-high an order. Such an approach was first proposed in Ref. [28] and further elaborated in papers [29–35].

The analysis of the dynamo equations in our case showed that if the dipole field demonstrates chaotic inversions, the quadrupole field is not constant and also evolving in a certain way in time, such that the strength of the quadrupole field at the instant of the dipole field inversion is random.

The study showed that the dynamo model reproduces the inversion regime under conditions when the value of some of the governing parameters fluctuates. In this model, the governing parameters include the amplitudes of differential rotation, the alpha-effect, and meridional flows. Notice that direct measurements of these physical characteristics are difficult, and in the models mainly their distribution with depth in the liquid core is estimated.

The alpha-effect manifests itself in the degree of mirror asymmetry of the convection, i.e., in the dominance of right eddies over left ones in one hemisphere, and vice versa in the other hemisphere. This left-and-right asymmetry arises in a stratified medium due to the action of the Coriolis force. Paper [36] suggested a qualitative explanation of how chirality fluctuations lead to the appearance of a long-term evolution of the geomagnetic field accompanied by numerous inversions. The results obtained in Ref. [36] were confirmed in study [34] proceeding from the low-mode approximation.

As model [26] takes into account meridional flows — the global convective flows of matter in the liquid outer core of Earth — we have checked how such flows can affect the inversion process. The analysis revealed that in the magnetic field vascillation regime (i.e., oscillations around a nonzero time average value), a drastic decrease in the meridional circulation amplitude by about 30% leads to magnetic field inversion.

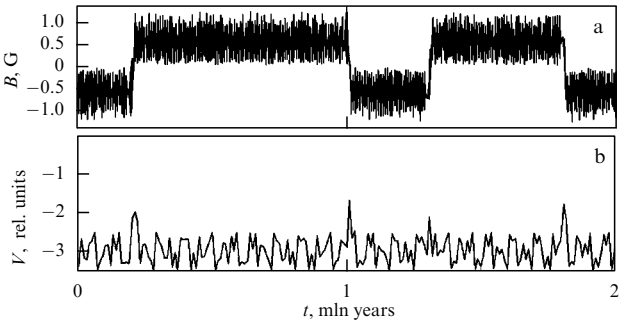

Figure 2. Mean dipole magnetic field strength on Earth's surface (a) and the velocity of the meridional motion of matter (b) as a function of time for the chaotic inversion regime.

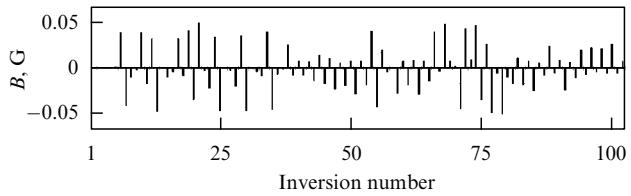

Figure 3. Maximum quadrupole field values on Earth's surface calculated in the geomagnetic dynamo model during 102 inversions.

Figure 2a plots the theoretical dependence of Earth's dipole field amplitude $B(t)$ as a function of time t based on the solution of the dynamo equations [26] for the regime of random inversions caused by meridional flow fluctuations. The timescale in this figure spans the interval from 0 to 2 mln years. The figure shows that large fluctuations of the meridional flows leading to inversion are rare, about once every several hundred thousand years. Figure 2b depicts the velocity $V(t)$ of the meridional flow of matter as a function of time t under the assumption that in the main part of the magnetic field generation region the meridional flows are directed oppositely to the magnetic field vector. Since in this paper we focus on the qualitative picture of magnetic field inversion mechanism, the meridional flows in Fig. 2 are remained in model units.

In our model, the value of the quadrupole magnetic field during the inversion of the dipole field is random. Figure 3 demonstrates the dispersion of the maximum quadrupole field amplitudes B across Earth's surface as the dipole field crosses zero for 102 consecutive inversions. It is seen that the quadrupole geomagnetic field strength on Earth's surface does not exceed approximately 0.05 G.

3. Problem setup. Numerical model

Our task is to study numerically the geomagnetic field evolution, to calculate the spectral change in the SCRs/GCRs penetrating into Earth's magnetosphere until they enter the atmosphere, and to estimate the radiation hazard at the ground level. To this end, we consider a spherical model region around Earth, in which the magnetic field $\mathbf{B}_{\text{Earth}}$ can be represented as a superposition of two components: the dipole one and the quadrupole one, taken with different weight coefficients. A layout of the model with Earth's quadrupole magnetosphere is shown in Fig. 4. Calculations have been carried out in the solar–magnetospheric coordinate system, in which the X-axis points from Earth's center towards the Sun,

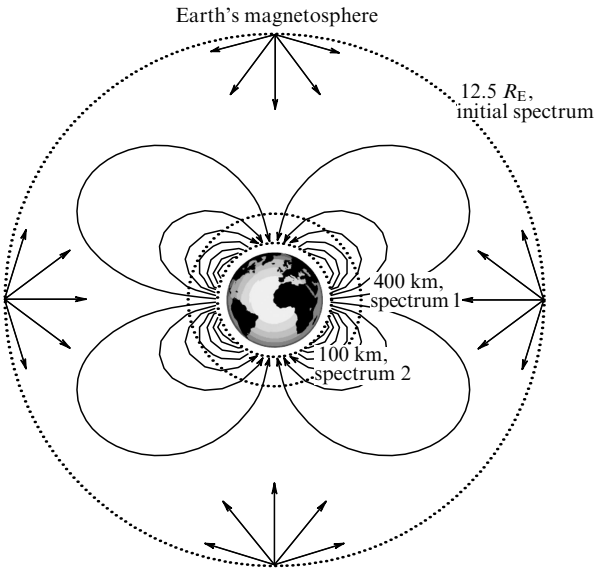

Figure 4. Layout of Earth's paleomagnetosphere. Shown are lines of force of the quadrupole magnetic field. The dashed curves indicate three levels at which particle energy spectra are calculated. At a distance of 12.5 R_E from Earth, the geomagnetic filed effect is small compared to the solar wind field; therefore, it is possible to set the initial GCR source on this conditional sphere with a given radius. The ISS trajectory passes at a distance of 400 km above the ground, (spectrum 1 GCR). In this region, part of the charged particle flux is cut off by Earth's magnetic field. Marked is the atmospheric boundary located 100 km above the ground (spectrum 2 GCR). The arrows show the directions of velocities of traced model particles.

the Y-axis is directed from the morning to the evening, and the Z-axis is coincident with the magnetic dipole axis prior to the inversion and is directed to the north.

An axially symmetric magnetospheric model is used, in which the ring and tail currents, as well as the effects of the radiation belts, can be ignored [17]. The interplanetary magnetic field $\mathbf{B}_{\rm IMF}$ in this model is not taken into account ($\mathbf{B}_{\rm IMF} = 0$). Model particles imitating SCR and GCR protons are ejected towards Earth from a spherical surface with a radius of 12.5 R_E centered on Earth (the approximate location of the present-day magnetopause in the head part of the magnetosphere). The initial energy distribution from 10 MeV to 100 GeV corresponds to the GCR [37] and SCR [38] spectra. Each particle was randomly ejected inside a cone with the axis passing through the starting point and Earth's center at opening angle $\pi/2$ and was traced in the given magnetic field $\mathbf{B}$, constant in time, ignoring electrical fields. Therefore, the particle's velocity module is conserved ($|\mathbf{v}| = \text{const}$), and the equation of motion of such a — generally speaking — relativistic particle in SI units has the form

$$\frac{\mathrm{d}\mathbf{r}}{\mathrm{d}t} = \mathbf{v}\,, \qquad m\,\frac{\mathrm{d}\mathbf{v}}{\mathrm{d}t} = Ze\sqrt{1-\frac{|\mathbf{v}|^2}{c^2}}\,\mathbf{v}\times\mathbf{B}\,. \tag{1}$$

This tracing enabled calculation of energy spectra of particles at distances of 400 km from Earth's surface, where the ISS trajectory passes, and at 100 km above the ground where the atmosphere boundary is located. The radiation hazard at ground level due to secondary particles from protons passing through the atmosphere was estimated. To validate the method, modeling in the present-day dipole field was carried out and the results were compared with radiation flux measurements performed at various altitudes in 2015.

Two inversion scenarios have been employed. The first assumed that the geomagnetic field at the moment of inversion represents a superposition of the residual dipole field with a strength of 10% of the present-day value and the quadrupole field. The second one assumed Earth's magnetic field to be purely quadrupole at the moment of inversion. The geomagnetic field $\mathbf{B}_{\rm Earth}$ was specified using the IGRF-12 model [39, 40]. The magnetic field potential U satisfies the Laplace equation $\Delta U = 0$, which has a solution in the form of a harmonic series:

$$U(r,\theta,\phi) = \sum_{n=0}^{\infty}\sum_{m=0}^{n}\frac{1}{r^n}\left[a_n^m\cos(m\phi) + b_n^m\sin(m\phi)\right]P_n^m(\cos\theta). \tag{2}$$

After normalizing the radial distance to Earth's radius R, we introduced the coefficients $g_n^m = a_n^m/R^{n+2}$ and $h_n^m = b_n^m/R^{n+2}$ to obtain

$$U(r,\theta,\phi) = R\sum_{n=1}^{\infty}\sum_{m=0}^{n}\left(\frac{R}{r}\right)^{n+1}\left[g_n^m\cos(m\phi) + h_n^m\sin(m\phi)\right] \times P_n^m(\cos\theta)\,. \tag{3}$$

Here r, θ, ϕ are geocentric coordinates, $g_n^m(t)$ and $h_n^m(t)$ are the Gauss coefficients generally depending on time t, and P_n^m are the Legendre polynomials of the nth power and mth order normalized according to the Schmidt rule:

$$P_n^0(x) = P_{n,0}(x)\,, \qquad P_n^m(x) = \left(\frac{2(n-m)!}{(n+m)!}\right)^{1/2}P_{n,m}(x)\,, \tag{4}$$

where

$$P_{n,m}(\cos\theta) = \sin^m\theta\,\frac{\mathrm{d}^m}{\mathrm{d}(\cos\theta)^m}\,P_n(\cos\theta)\,.$$

The corresponding magnetic field components $\mathbf{B} = -\nabla U$ are expressed as

$$B_r = -\frac{\partial U}{\partial r}\,, \quad B_\theta = -\frac{1}{r}\frac{\partial U}{\partial\theta}\,, \quad B_\phi = -\frac{1}{r\sin\theta}\frac{\partial U}{\partial\phi}\,, \tag{5}$$

$$B_r = \sum_{n=1}^{\infty}\sum_{m=0}^{n}\left(\frac{R}{r}\right)^{n+2}(n+1)\left[g_n^m\cos(m\phi) + h_n^m\sin(m\phi)\right] \times P_n^m(\cos\theta)\,,$$

$$B_\theta = -\sum_{n=1}^{\infty}\sum_{m=0}^{n}\left(\frac{R}{r}\right)^{n+2}\left[g_n^m\cos(m\phi) + h_n^m\sin(m\phi)\right] \times \frac{\partial P_n^m(\cos\theta)}{\partial\theta}\,,$$

$$B_\phi = -\frac{1}{\sin\theta}\sum_{n=1}^{\infty}\sum_{m=0}^{n}\left(\frac{R}{r}\right)^{n+2}m\left[-g_n^m\sin(m\phi) + h_n^m\cos(m\phi)\right] \times P_n^m(\cos\theta)\,. \tag{6}$$

As described above, we represent the geomagnetic field as a superposition of the dipole and quadrupole components:

$$\mathbf{B}_{\rm Earth} = \mathbf{B}_{\rm dip} + \mathbf{B}_{\rm quadrup}\,. \tag{7}$$

The first three terms of the magnetic dipole $\mathbf{B}_{\rm dip}$ decomposition have the form

$$B_r^{\rm dip} = 2\left(\frac{R}{r}\right)^3 \left[g_1^0 \cos\theta + (g_1^1 \cos\phi + h_1^1 \sin\phi)\sin\theta\right],$$

$$B_\theta^{\rm dip} = -\left(\frac{R}{r}\right)^3 \left[-g_1^0 \sin\theta + (g_1^1 \cos\phi + h_1^1 \sin\phi)\cos\theta\right], \quad (8)$$

$$B_\phi^{\rm dip} = -\left(\frac{R}{r}\right)^3 (-g_1^1 \sin\phi + h_1^1 \cos\phi).$$

The magnetic quadrupole $\mathbf{B}_{\rm quadrup}$ can be represented as follows:

$$B_r^{\rm q} = 3\,\frac{\sqrt{3}}{2}\left(\frac{R}{r}\right)^4 \left\{g_2^0\,\frac{3\cos^2\theta - 1}{\sqrt{3}} + (g_2^1 \cos\phi + h_2^1 \sin\phi) \times \sin(2\theta) + \left[g_2^2 \cos(2\phi) + h_2^2 \sin(2\phi)\right]\sin^2\theta\right\},$$

$$B_\theta^{\rm q} = -\frac{\sqrt{3}}{2}\left(\frac{R}{r}\right)^4 \left\{-g_2^0\sqrt{3}\sin(2\theta) + (g_2^1 \cos\phi + h_2^1 \sin\phi) \times 2\cos(2\theta) + \left[g_2^2 \cos(2\phi) + h_2^2 \sin(2\phi)\right]\sin(2\theta)\right\}, \quad (9)$$

$$B_\phi^{\rm q} = -\frac{\sqrt{3}}{2}\left(\frac{R}{r}\right)^4 \frac{1}{\sin\theta}\left\{(-g_2^1 \sin\phi + h_2^1 \cos\phi)\sin(2\theta) + \left[-2g_2^2 \sin(2\phi) + 2h_2^2 \cos(2\phi)\right]\sin^2\theta\right\}.$$

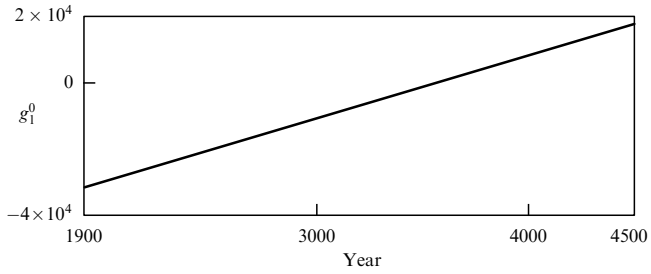

Figure 5. Extrapolation in time of the leading dipole coefficient g_1^0.

The coefficients g and h as functions of time during the period from 1900 till 2020 are known from the IGRF-12 model. Presently, the dipole coefficients g_1^0, g_1^1, h_1^1 decrease with time, and the quadrupole ones, g_2^0, g_2^1, g_2^2, h_2^1, h_2^2, increase. We have extrapolated the leading dipole coefficient up to the year 4500 (Fig. 5). The figure suggests that by the year 3580 the leading dipole coefficient will have vanished, i.e., assuming a constant dipole field decay rate, magnetic field inversion should occur.

Figure 6 depicts the surface magnetic field module as a function of latitude and longitude. All fields were then computed with the Gauss coefficients obtained for the year 2015. Figure 6a plots multipole components of the geomagnetic field through the 5th order, and Fig. 6b shows multi-

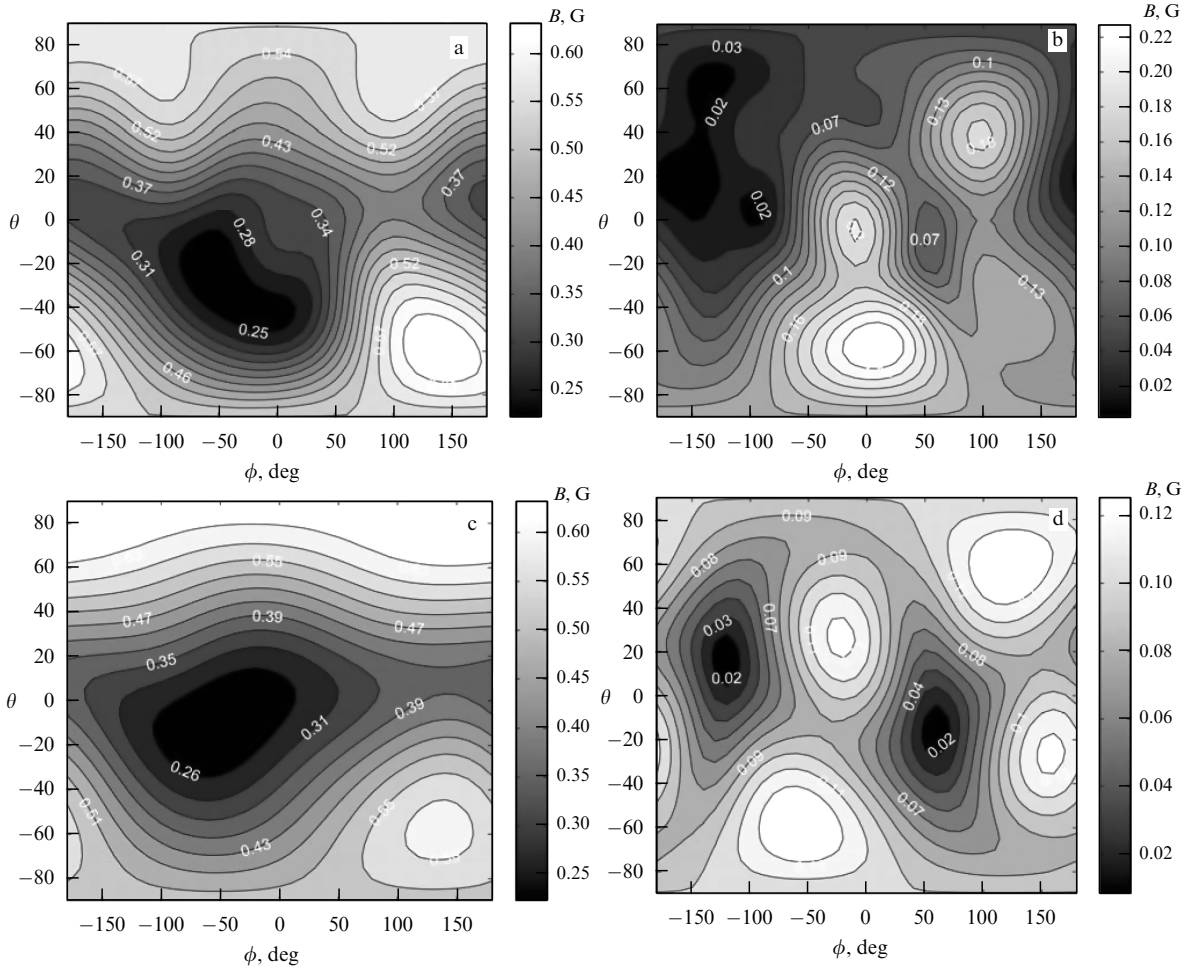

Figure 6. Magnetic field induction B [G] distribution across latitude θ and longitude ϕ with coefficients as of 2015: (a) the multipole magnetic field up to the 5th order inclusive; (b) the same multipoles but without the dipole component; (c) superposition of the dipole and quadrupole; (d) quadrupole.

poles without the dipole component. As noted above, the higher the order of the multipole component, the faster it decays with distance. Therefore, we restricted ourselves by considering a combination of the first two components: the dipole and quadrupole ones. Figure 6c demonstrates the field containing only the dipole and quadrupole, and Fig. 6d shows the quadrupole field (it is assumed that during the magnetic inversion expected around the year 3600 the dipole field will have fully disappeared). It can also be noted that the magnetic field strengths with multipoles up to the 5th order inclusive (Fig. 6a) and up to the 2nd order inclusive (Fig. 6c) do not differ significantly. We will also consider a superposition of the 10% dipole and quadrupole fields. Such an inversion with the incomplete disappearance of the dipole component has been assumed in some papers [15, 17].

4. Radiation environment in the near-Earth space and on the ground

As the GCR particle energies are on average a few orders of magnitude higher than those of SCRs and most of them (92%) are protons, we will assume that the radiation environment near Earth is mainly determined by GCR protons and EAS particles produced by the interaction of GCR protons with the atmosphere. Figure 7 presents the model logarithmic spectra of the GCR particles (protons p^+, electrons e^-, helium ions $^4_2He^+$, and oxygen ions $^{16}_8O^+$) outside Earth's magnetosphere. It is seen that the flux density of GCR protons with energies above 30 MeV significantly exceeds those of other GCR particles. Therefore, we have ignored in the present paper contributions from GCR electrons and heavy ions to the radiation environment on Earth. It is also known [46] that protons with energies below the pion creation threshold (~ 300 MeV) lose energy in atmospheric interactions for ionization and excitation of atomic nuclei in the air. With decreasing energy, the effective cross section of proton ionization losses increases. As a result, all low-energy protons are rapidly decelerated and absorbed. Thus, to estimate the radiation dose on Earth's surface, only GCR protons with energies above 300 MeV will be considered.

The radiation situation in the ISS orbit is somewhat different: it requires taking into account the effect of GCR and SCR protons. The electron flux density has been ignored again, because electrons are much less dangerous than protons due to different mechanisms of their impact on humans [46].

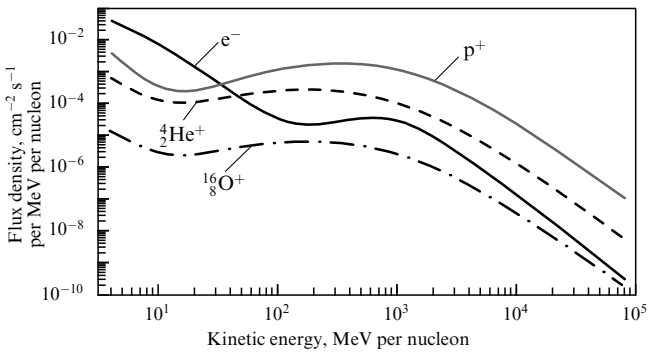

Figure 7. Mean differential spectra of GCR particles: protons (p^+), electrons (e^-), helium ions ($^4_2He^+$), and oxygen ions ($^{16}_8O^+$) at a distance of 12.5 R_E outside the magnetosphere.

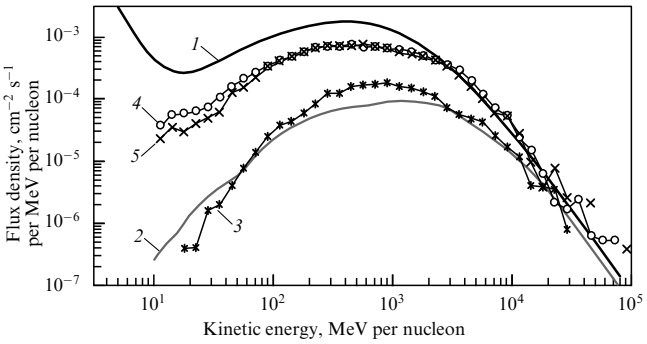

Figure 8. Experimental mean differential spectra of GCR protons at the solar activity minimum: in Earth's orbit outside the magnetosphere (curve *1*), in the ISS orbit at latitude $\theta = 51.6°$ (curve *2* reflects observational data), and the spectra calculated at the altitude of 400 km and latitudes $\theta = 50° - 55°$ for the present-day field configuration (curve *3*) and at the moment of inversion: 10% dipole + quadrupole (curve *4*) and pure quadrupole (curve *5*).

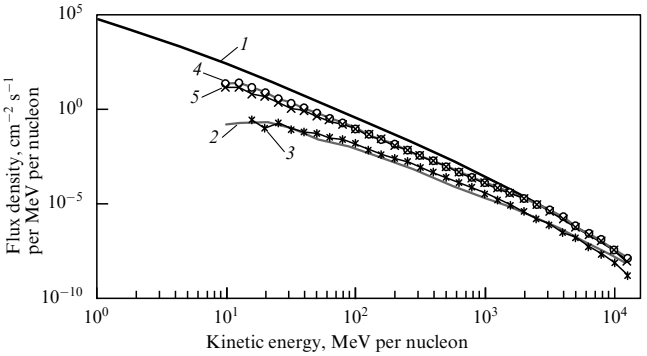

Figure 9. Experimental mean differential spectra of SCR protons at the solar activity maximum: in Earth's orbit outside the magnetosphere (curve *1*), in the ISS orbit at latitude $\theta = 51.6°$ (experimental curve *2*), as well as the model spectra calculated at the altitude of 400 km and latitudes $\theta = 50° - 55°$ for the present-day field configuration (curve *3*) and at the moment of inversion: 10% dipole + quadrupole (curve *4*) and pure quadrupole (curve *5*).

To verify the model particle energy spectra, a comparison of the calculated and observed spectra in the present-day magnetic field (2015) was performed, in particular, with measurements carried out at the ISS (2015). The differential GCR and SCR proton spectra were calculated at different distances from the Earth using the model with the corresponding source spectra on the 12.5 R_E sphere. The calculated spectra were compared at the altitude of 400 km and latitudes $50° - 55°$ with the ISS data obtained at the 400 km altitude and $\theta = 51.6°$ latitude. The obtained spectra are presented in Figs 8 and 9. The figures demonstrate that the calculated spectra (curves *3*) corresponding to present-day conditions are in a rather good agreement with the ISS data (curves *2*). Thus, we can conclude that the model quite adequately calculates the high-energy particle fluxes penetrating into Earth's magnetosphere from interplanetary space.

Figure 10 displays regions available for GCR protons at an altitude of 100 km above sea level before field inversion (Fig. 10a) and during the inversion: the inversion scenario shown in Fig. 10b includes 10% of the dipole field and 90% of the quadrupole field, while in Fig. 10c only the quadrupole field is present.

Clearly, the disappearance of the dipole component should change not only the 'geography' of particle precipita-

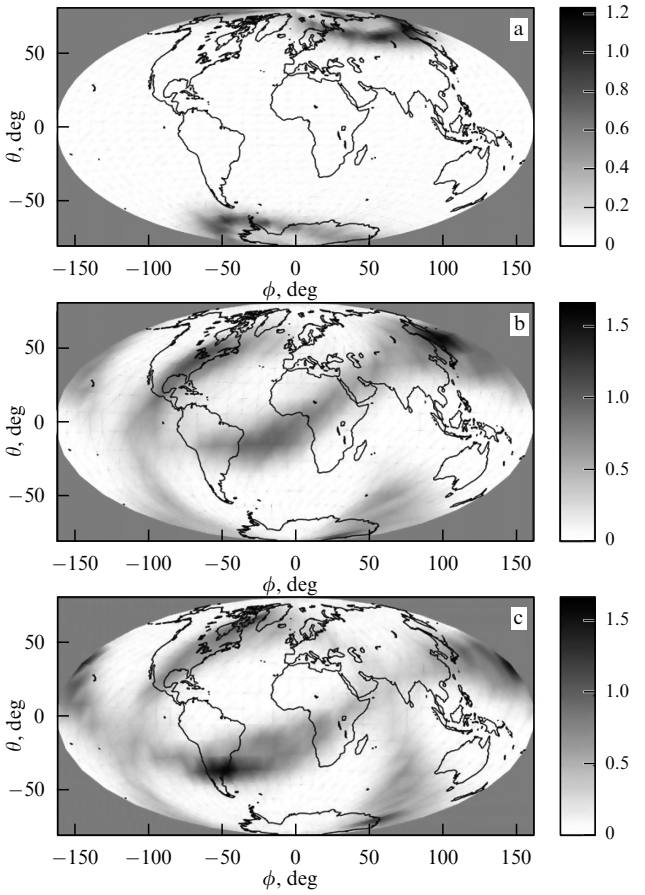

Figure 10. Percent ratio of protons on the ground to the total number of protons hitting Earth's atmosphere boundary (100 km) (a) in 2015; in the inversion scenarios with (b) 10% dipole and 90% quadrupole field; (c) in the pure quadrupole field.

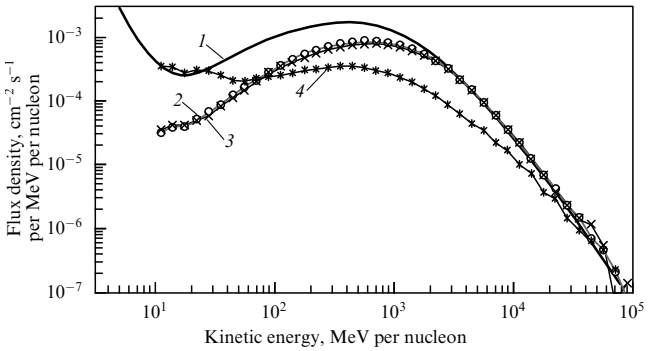

Figure 11. Mean differential spectra of GCR protons at the solar activity minimum at a distance of 12.5 R_E from Earth's center outside the magnetosphere (curve *1*), at a distance of 100 km above the ground level for the magnetic field inversions (curves *2*, *3* correspond to scenarios presented in Figs 10b, c, respectively), and in 2015 (curve *4*).

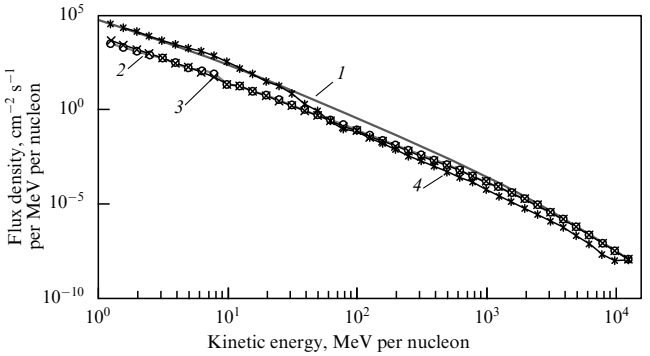

Figure 12. Mean differential spectra of SCR protons at the solar activity maximum at a distance of 12.5 R_E from Earth's center outside the magnetosphere (curve *1*), at a distance of 100 km above ground level for the magnetic field inversions (curves *2*, *3*), and in 2015 (curve *4*).

tion but also the number of particles. The increase in the number of protons and their precipitation zone area at the moment of field inversion suggests a worsening of the radiological hazard in the circumterrestrial space. In Fig. 10c (pure quadrupole), one can also see the penetration of particles into the South Atlantic Anomaly (SAA) region — the region with the weakest modern geomagnetic field, less than 0.32 G at sea level. The SAA is located in the latitude interval from $-50°$ to $0°$, and at longitudes from $-90°$ to $+40°$ (Fig. 6a). However, at the moment of inversion, the magnetic field topology would be such that the SAA would have a higher magnetic field strength (Fig. 6b), and the particle flux there would increase.

In passing through the atmosphere, the number of 'primary' protons decreases due to nuclear interactions and ionization losses, but interactions of the high-energy 'primary' protons with nuclei generate a certain number of 'secondary' protons, because a destroyed nucleus decays into protons and neutrons with lower energies [41, 42]. The results reported in Refs [43, 44] suggest that positive and negative muons, as well as neutrons generated by nuclear interactions, mostly contribute to the radiation exposure dose. Below, we provide estimates of the radiation situation on Earth due to secondary particles, which are virtually independent of the magnetic field strength.

Figures 11 and 12 illustrate the mean energy spectra of GCR and SCR protons at the entrance to Earth's magnetosphere and upon entering the atmosphere: at a distance of 12.5 R_E from Earth's center (curve *1*), at a distance of 100 km from the ground in the year 2015 (curve *4*), and for two possible field configurations at the moment of magnetic inversion (curves *2*, *3* correspond to scenarios shown in Figs 10b, c, respectively). The mean energy spectra of these two inversions were found to be identical, although the particle spatial precipitation regions (Figs 10b, c) are different.

Figures 11 and 12 suggest that in 2015 the GCR and SCR proton fluxes in the circumterrestrial space with energies below 100 MeV exceed those at the inversion moment. However, as discussed above, they do not contribute to the radiation exposure on the ground. Therefore, the part of the spectrum below 300 MeV (the pion creation threshold) has been ignored in calculations of the radiation on Earth's surface.

A comparison with Fig. 10a shows that in the near-Earth space (100–400 km) with an account for the low-energy spectrum (below 100 MeV) the mean radiation background turns out to be higher in the present-day magnetic field than during inversion due to the presence of high-latitude zones with enhanced radiation exposure. At the same time, at the ISS latitudes, the proton flux density at the inversion moment should still be higher than in 2015 (see Figs 8 and 9).

It is possible to explain the increase in the GCR and SCR proton fluxes at low energies for the 2015 magnetic field as

Table 1. Radiation dose power [mSv day^{-1}] in the ISS orbit for three magnetic field configurations and without a magnetic field at the solar activity maximum.

	2015 field	10% dipole + quadrupole	0% dipole + quadrupole	Without magnetic field
GCR	0.23	0.77	0.87	1.08
SCR	1.45	15.56	22.28	113.7
GCR + SCR	1.68	16.33	23.15	114.8

Table 2. Radiation dose power [mSv day^{-1}] in the ISS orbit for three magnetic field configurations and without a magnetic field at the solar activity minimum.

	2015 field	10% dipole + quadrupole	0% dipole + quadrupole	Without magnetic field
GCR	0.37	1.3	1.4	2
SCR	0.04	0.42	0.62	3.26
GCR + SCR	0.41	1.72	2	5.26

Table 3. Radiation dose power [mSv day^{-1}] from protons with energies of > 300 MeV at an altitude of 100 km from the ground for three magnetic field configurations and without a magnetic field during the solar activity maximum.

	2015 field	10% dipole + quadrupole	0% dipole + quadrupole	Without magnetic field
GCR	0.27	0.68	0.73	0.97
SCR	0.31	0.6	0.67	1.9
GCR + SCR	0.58	1.28	1.4	3.9

Table 4. Radiation dose power [mSv day^{-1}] from protons with energies of > 300 MeV at an altitude of 100 km from the ground for three magnetic field configurations and without a magnetic field during the solar activity minimum.

	2015 field	10% dipole + quadrupole	0% dipole + quadrupole	Without magnetic field
GCR	0.46	1.25	1.31	1.87
SCR	0.006	0.011	0.012	0.035
GCR + SCR	0.47	1.26	1.32	1.91

follows. Let us estimate at which distance r^* from Earth's center the external magnetic field is capable of significantly changing the initial (without the magnetic field) trajectories of charged particles, such that they could reach the given altitudes over the ground level. Since the dipole magnetic field strength decreases with distance more slowly than the quadrupole field strength does, the number of magnetized low-energy particles in the modern magnetic field (dominated by the dipole component) is higher than during the magnetic field inversion. The magnetization criterion can be formulated as the inequality $R_{\mathrm{Larm}}(r^*)/r^* \leqslant 1$, where $R_{\mathrm{Larm}}(r^*) = mv_\perp/(eB(r^*))$ is the Larmor radius of the rotating particle, and r^* is its radial distance from Earth's center.

The upper estimates of r^* being sought for can be obtained by simple numerical tracing of particles with energies below 10 MeV (the least energetic in the range considered): $r^*_{\max} \approx 21.5\,R_{\mathrm{E}}$ in the 2015 magnetic field, and $r^*_{\max} \approx 9\,R_{\mathrm{E}}$ and $r^*_{\max} \approx 5\,R_{\mathrm{E}}$ in inversion fields consisting of 10% of the dipole and quadrupole and pure quadrupole, respectively. These estimates imply that the modern magnetic filed can magnetize low-energy protons at large distances. The magnetized protons cannot go into the outer magnetosphere and then escape into the interplanetary space, but can be captured in spiral trajectories and, by moving along magnetic field lines at high latitudes, can precipitate to Earth, which increases their flux density. However, in the quadrupole field, a large number of particles with energies of < 100 MeV do not hit Earth but escape into the outer magnetosphere and ultimately into the interplanetary magnetic field.

Let us assess the biological impact of GCR protons. To do this, let us represent the formula for the effective radiation dose power [45] in the form

$$H_R = \frac{1}{\rho}\int \Phi(E)\,Q(E)\,\frac{\mathrm{d}E}{\mathrm{d}x}\,\mathrm{d}E\,, \tag{10}$$

where $Q(E)$ is the quality coefficient of the ionizing radiation (GOST 8.496-83 GSI), ρ is the density of the medium, $\mathrm{d}E/\mathrm{d}x$ is the ionization losses described by the known formula [46], and $\Phi(E)$ is the differential particle energy spectrum. The differential spectra used in the calculations are represented in Figs 8, 9, 11, and 12. Here, in Figs 8 and 11 are shown GCR proton spectra during the solar activity (SA) minimum at altitudes of 400 km (in the ISS orbit) and at 100 km above the ground level, and in Figs 9 and 12 are presented SCR proton spectra at the SA maximum at the same altitudes. These spectra are chosen such because the maximum radiation doses on the ground level are found during the SA minima due to GCR particles, and in the ISS orbit due to SCR particles during SA maxima.

The calculated effective radiation doses caused by GCR and SCR protons are listed in Tables 1–5, according to which, the GCR and SCR proton flux densities are higher for the pure quadrupole field than for a superposition of 10% of the dipole and quadrupole fields; therefore, below we will assume a pure quadrupole field during the magnetic field inversion.

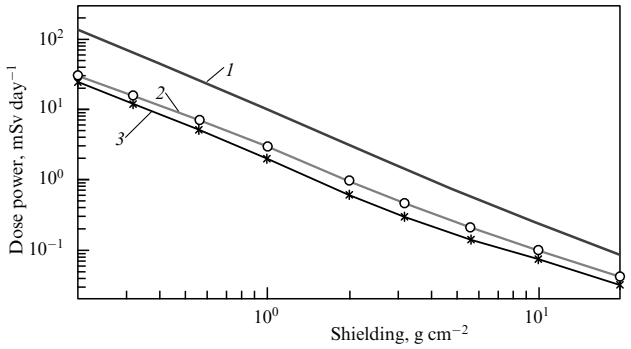

Figure 13. Average power of an equivalent radiation dose under different shieldings at the SA maximum in the ISS orbit caused by radiation belt, SCR, and GCR particles (curve *3*), and due to SCRs and GCRs without the magnetosphere (curve *1*), and in a quadrupole field (curve *2*).

Table 5. Corrected radiation dose power [mSv yr^{-1}] on Earth's surface for three magnetic field configurations and without a magnetic field (during the solar activity minimum).

2015 field	10% dipole + quadrupole	0% dipole + quadrupole	Without magnetic field
0.3	0.8	0.85	1.2

Table 6. Impact of γ-radiation dose on humans.

Dose, mSv	Impact on humans
0 – 200	No visible damage
200 – 500	Possible changes in blood composition
500 – 1000	Change in blood composition, damage
1000 – 2000	Damage, possible incapacitation
2000 – 4000	Total disability, possible fatality
4000	50% mortality
6000	Lethal

In the ISS orbit, SCR protons mainly contribute to the radiation dose during the SA maximum (86% of the total radiation dose power from GCRs and SCRs for the modern field, and 97% for the pure quadrupole field). Table 1 suggests that during inversion the total radiation dose power is 23.2 mSv day^{-1} (or 8500 mSv yr^{-1}). According to Table 6, these doses accumulated in one year would exceed the permissible radiation limit of 200 mSv, which can significantly restrict the duration of stay of astronauts in orbit, even with account for shielding. Figure 13 shows the radiation dose power decrease with shielding thickness (from the space suit to the ISS outer sheet).

The radiation background in the ISS during the SA minimum is quite different. The SCR proton spectra at the SA minimum are one and a half orders of magnitude below those at the SA maximum plotted in Fig. 8. The calculations showed (see Table 2) that at the moment of inversion, the total radiation dose power would be 2 mSv day^{-1} (or 730 mSv yr^{-1}).

Table 3 presents calculations of radiation dose powers averaged over the planet surface from GCR and SCR protons with energies above 300 MeV at an altitude of 100 km. At this altitude, GCR and SCR particles almost equally contribute to the radiation background for both the modern magnetic field and the field during magnetic inversion. However, the radiation situation on Earth's surface is mainly determined by high-energy GCR protons, whose dose at the altitude of 100 km, as seen from Tables 3 and 4, during the SA maximum is two times as low as during the minimum. Correspondingly, the same ratio of radiation doses can be expected on the ground.

Table 4 presents the radiation power doses for GCR and SCR protons with energies above 300 MeV at the altitude of 100 km during the SA minimum. As expected, the SCR particles do not significantly contribute in this case to the total radiation background.

To estimate the radiation dose power on the ground level, we calculate the radiation dose ratio at the altitude of 100 km for the inversion ($H_{R3} = 1.32$ mSv day^{-1}) and modern (2015) ($H_{R2} = 0.47$ mSv day^{-1}) fields: $H_{R3}/H_{R2} \approx 3$. By assuming that Earth's magnetic field is zero ($H_{R3} = 1.9$ mSv day^{-1}), the corresponding radiation dose power ratio would be $H_{R1}/H_{R2} \approx 4$. By approximately setting constant atmospheric properties, we can assume that the obtained coefficient will be conserved on Earth's surface at the time of inversion, too.

According to the PARMA model (PHITS-based Analytical Radiation Model in the Atmosphere; PHITS — Particle and Heavy Ion Transport code System), to estimate CR fluxes [44], in 2015 at the solar activity minimum the human radiation exposure at sea level due to cosmic rays was about 8×10^{-4} mSv day^{-1}, or 0.3 mSv yr^{-1}. From Table 6 showing the impact of the yearly radiation dose on humans, it is possible to conclude that a three- or even a four-fold increase in this dose will not be dangerous for humans over the natural duration of the human life ($\leqslant 100$ years). For completeness, the assumed radiation dose powers on Earth's surface at the SA minimum are taken into account in Table 5.

5. Discussion

The geomagnetic field inversion process, which has likely started at present, can affect the structure of Earth's magnetosphere, the radiation situation [47, 48], and life on Earth in general [9, 10, 16, 49, 50]. During the inversion, in addition to the dipole component reversal, a shift of the quadrupole component is possible. In this case, the magnetic anomalies will change location, which also contributes to the cosmic radiation redistribution on Earth.

Paper [49] assumed that during the magnetic inversion period particles from the Sun hitting Earth are barely deflected by the magnetic field, and these particles, together with particle precipitations from the Van Allen belts, would make further life on Earth impossible. However, later paper [50] argued against this possibility, because, even if the geomagnetic field was totally absent, no impact of energetic particles on the biosphere should be expected, since the atmosphere effectively absorbs the primary particles of solar and cosmic origin. This statement was confirmed by measurements in Ref. [10] revealing that at altitudes from 18 to 12 km above sea level the equivalent radiation dose due to cosmic particles decreases by about a factor of two, and at altitudes from 12 to 6 km it decreases by about a factor of 7–10. Therefore, the atmosphere plays the role of a reliable shield against primary cosmic particles.

However, atmospheric screening is not yet perfect; therefore, the impact of the magnetic field inversion on humans on

Earth remains an open issue. The problem should be considered taking into account all factors determining the conditions for life on Earth [8–10, 51, 52]. The consequences of magnetic inversion could also include, in addition to higher radiation dose, ozone layer exhaustion [53–56] and various climatic changes on Earth [51, 57]. Paper [58] argues that such an important part of the magnetosphere as radiation belts should disappear when the dipole field would be minimized during magnetic field inversion, with only the quadrupole component surviving. Some authors have found sufficiently compelling correlations between magnetic epochs/episodes and mass extinctions of living creatures on Earth [9, 10, 47, 48] and glacial epochs [59]. Apparently, the causal connections between life and the geomagnetic field are indirect and involve chains of different processes [60, 61]. The magnetic field polarity change is shown to be well correlated with periods of raised extinction of some living organisms and the appearance of new species [62, 63]. The correlation between the polarity change and plant boundaries on the Earth was also confirmed [64].

Thus, the impact of inversions on the biosphere and on humans, in particular, can be significant, although it is quite possible that such changes appear on paleomagnetic timescales and not during the lifetime of an individual or even the span of several generations.

Unlike low-energy SCRs, during the geomagnetic dipole field disappearance, high-energy SCR fluxes will be much higher inside Earth's magnetosphere and will provide larger radiation exposures to the ground. A long-term period of increased radiation lasting one thousand years or even more could be dangerous for humankind, its technological environment, and near-Earth space expeditions. The question is: can humankind survive in the periods of increased radiation fluxes during magnetic inversions?

To elucidate this issue, we have carried out numerical simulations to estimate radiation threats for humans from GCR and SCR fluxes on the ground and at the ISS altitude of 400 km during an inversion period, when, according to the hypothesis, the dipole component of the geomagnetic field should totally or partially disappear. The model results and their analysis suggest that for the ISS orbiting at 400 km SCR particles, whose flux should increase by a factor of 14 over the present-day value, are the most dangerous.

Thus, radiation exposure to astronauts could be as high as 6000 mSv yr^{-1} or 8500 mSv yr^{-1} (without shielding) at the SA maximum. Most of the low-energy solar wind particles will be absorbed by the atmosphere and will not reach Earth's surface. At the same time, the radiation at the ground level should increase due to secondary GCRs (muons) and photon radiation, to which the atmosphere is transparent.

By assuming constant atmospheric properties by the beginning of inversion epoch, it is possible to predict a three-fold radiation increase at the solar activity minimum and a two-fold increase at the solar activity maximum. However, taking into account the present SA minimum radiation level at sea level of 8.02×10^{-4} mSv day^{-1}, a three-fold increase in the radiation background should not be dangerous for humans. Nevertheless, there is no certainty that on the full inversion timescale of 5–10 thousand years the elevated radiation background is totally safe for humans and organic life on Earth. It cannot be ruled out that the accumulation of genetic mutations [65–67] could have remote effects and appear on a longer timescale on the order of the inversion duration or longer.

To conclude, we can say that the results of our calculations, on the one hand, disprove studies arguing a significant heightened radiation impact on all living organisms on Earth at the period of magnetic field inversion: no critical radiation background rise has been found. At the same time, our results have a preventive character suggesting a radiation danger for humans in space (for example, in orbital stations at certain latitudes of $< 60^\circ$) during magnetic inversion periods.

6. Conclusion

In the present paper, we considered a possible scenario of the disappearance of the dipole component of the geomagnetic field during Earth's magnetic dipole inversion. An $\alpha\Omega$-dynamo model for the dipole and quadrupole field components was constructed. We considered two possible inversion scenarios: (1) with quadrupole and 10%-dipole magnetic fields, and (2) only with a quadrupole field. For both scenarios, we calculated GCR and SCR proton spectra and their flux distributions across Earth and estimated the change in the effective proton radiation doses.

We have shown that, assuming constant atmospheric properties, the mean effective doses of GCR protons (SCR protons make a minor contribution) should increase about three-fold over the 2015 level. It has been shown that the magnetic field configuration change will result in the redistribution of higher radiation regions over Earth's surface (these regions are now located around the North and South Magnetic Poles), which can have negative effects on the health of the human population in these regions.

On Earth, the radiation mainly caused by GCR particles inversely correlates with solar activity periods, i.e., it reaches a maximum during the solar activity minimum. As for the ISS, the maximum radiation caused by SCR and GCR particles correlates with the maximum solar activity, because SCR particles mainly contribute to the radiation environment in the ISS orbit. Estimates show that during an inversion at the maximum solar activity the power of SCR and GCR effective doses in the ISS orbit (at the latitude of 51.6° and altitude of 400 km) should increase by a factor of 14 compared to the 2015 level, which is due to the latitudinal redistribution of the radiation. Here, the general radiation background at the 400-km altitude during inversion can be a factor of 4.5 lower than the present-day value because of the decrease in the capture rate of the low-energy SCR component by the Earth's lower-sized quadrupole magnetosphere.

The main problem discussed in the present paper was the reality of an increased radiation hazard for humans on Earth during a magnetic field inversion. The results obtained give a negative answer. Indeed, although, on average, the radiation background should increase by a factor of about three during the solar minimum period, and the elevated radiation regions should be redistributed and their areas will apparently increase due to the dipole field decrease, such radiation doses are not dangerous for humans and other living creatures. At the same time, for astronauts aboard the ISS orbiting at 400 km above the ground, during an inversion period a 14-fold radiation increase can be dangerous. Undoubtedly, in this case, a correction of the orbits of space vehicles would be required.

It should be stressed that the issues of the impact of elevated radiation dose on Earth's biosphere and the long-term evolution of the magnetosphere during magnetic inversions remain poorly understood and require more in-

depth studies. A detailed consideration of the radiation environment on the ground and in the near-Earth space, taking into account different scenarios of the magnetic field change in time, will be presented by the authors in further studies.

Acknowledgments

The authors deeply acknowledge the Director of the Skobeltsyn Institute of Nuclear Physics of Lomonosov Moscow State University M I Panasyuk, I I Alekseev, V V Kalegaev, S I Svertilov, and V I Galkin for fruitful discussions of the present paper results and valuable suggestions. The authors thank V V Bengin (Institute of Biomedical Problems of RAS) and Jordanka Semkova (Space Research and Technology Institute, Bulgarian Academy of Sciences) for consultations about radiation dose calculations.

The work of LMZ is supported by the Russian Foundation for Basic Research (RFBR) grants 16-02-00479 and 16-52-16009-NTsNIL-a. The work of EPP is supported by the Russian Science Foundation grant 16-17-10097. The work of MVP is supported by RFBR grant 17-29-01022.

References

1. Vine F J, Matthews D H *Nature* **199** 947 (1963)
2. Gubbins D *Rev. Geophys.* **32** 61 (1994)
3. Korte M, Mandea M *Earth Planets Space* **60** 937 (2008)
4. Jacobs J A *Reversals of the Earth's Magnetic Field* (New York: Cambridge Univ. Press, 1994)
5. Gubbins D, Kelly P *J. Geophys. Res.* **100** 14955 (1995)
6. Soler-Arechalde A M et al. *Front. Earth Sci.* **3** 11 (2015)
7. Sagnotti L et al. *Geophys. J. Int.* **199** 1110 (2014)
8. Glassmeier K-H et al. *Int. J. Astrobiol.* **8** 147 (2009)
9. Glaßmeier K-H, Soffel H, Negendank J F W, in *Geomagnetic Field Variations* (Advances in Geophysical and Environmental Mechanics and Mathematics, Eds K-H Glaßmeier, H Soffel, J F W Negendank) (Berlin: Springer-Verlag, 2009) p. 1
10. Glassmeier K-H, Vogt J *Space Sci. Rev.* **155** 387 (2010)
11. Hoffman K A *Nature* **359** 789 (1992)
12. Kida S, Araki K, Kitauchi H *J. Phys. Soc. Jpn.* **66** 2194 (1997)
13. Olson P, Driscoll P, Amit H *Phys. Earth Planet. Inter.* **173** 121 (2009)
14. Sheyko A, Finlay C C, Jackson A *Nature* **539** 551 (2016)
15. Vogt J et al. *J. Geophys. Res.* **109** A12221 (2004)
16. Glassmeier K-H et al. *Ann. Geophys.* **22** 3669 (2004)
17. Stadelmann A et al. *Earth Planets Space* **62** 333 (2010)
18. Maksimochkin V I, Tselebrovskii A N, Shreider A A *Uch. Zap. Fiz. Fak. Mosk. Gos. Univ.* **3** 1631910 (2016)
19. Schmidt A *Gerlands Beiträge Geophys.* **41** 346 (1934)
20. Merrill R T, McFadden P L *Rev. Geophys.* **37** 201 (1999)
21. Valet J, Meynadier L *Nature* **366** 234 (1993)
22. Williams I, Fuller M *J. Geophys. Res.* **86** 11657 (1981)
23. Clement B M, Kent D V *Phys. Earth Planet. Inter.* **39** 301 (1985)
24. Clement B M *Earth Planet. Sci. Lett.* **104** 48 (1991)
25. Bradford M C, Kent D V *J. Geophys. Res.* **89** 1049 (1984)
26. Popova H *J. Phys. Conf. Ser.* **681** 012021 (2016)
27. Popova E P *Phys. Usp.* **59** 513 (2016); *Usp. Fiz. Nauk* **186** 577 (2016)
28. Ruzmaikin A A *Comm. Astrophys.* **9** 85 (1981)
29. Kitiashvili I, Kosovichev A G *Astrophys. J.* **688** L49 (2008)
30. Kitiashvili I, Kosovichev A G *Geophys. Astrophys. Fluid Dyn.* **103** 53 (2009)
31. Sokolov D D, Nefedov S N *Vychisl. Metody Programmirovanie* **8** 195 (2007)
32. Nefedov S N, Sokoloff D D *Astron. Rep.* **54** 247 (2010); *Astron. Zh.* **87** 278 (2010)
33. Sokoloff D D et al. *Astron. Lett.* **34** 761 (2008); *Pis'ma Astron. Zh.* **34** 842 (2008)
34. Sobko G S et al. *Geomagn. Aeronom.* **52** 254 (2012); *Geomagn. Aeronom.* **52** 271 (2012)
35. Popova H *Magnetohydrodynamics* **49** 59 (2013)
36. Hoyng P *Astron. Astrophys.* **272** 321 (1993)
37. ISO 15390:2004. Space environment (natural and artificial) – Galactic cosmic ray model, https://www.iso.org/standard/37095.html
38. Nymmik R A *Kosmich. Issled.* **31** 51 (1993)
39. Thébault E, Finlay C C, Toh H *Earth Planets Space* **67** 158 (2015)
40. Thébault E et al. *Earth Planets Space* **67** 79 (2015)
41. Galper A M *Kosmicheskie Luchi* (Cosmic Rays) (Moscow: MIFI, 2002)
42. Kalmykov N N, Kulikov G V, Roganova T M, in *Model' Kosmosa* (Model of Cosmos) Vol. 1 (Ed. M I Panasyuk) (Moscow: KDU, 2007) p. 62
43. Sato T et al. *Radiat. Res.* **170** 244 (2008)
44. Sato T *PLoS ONE* **10** e0144679 (2015)
45. Dietze G, in *Proc. of the IRPA-10, 10th Intern. Congress of the Intern. Radiation Protection Association, 14 – 19 May 2000, Hiroshima, Japan* (Hiroshima: IRPA, 2000) p. EO-3
46. Antonov R A, in *Model' Kosmosa* (Model of Cosmos) Vol. 1 (Ed. M I Panasyuk) (Moscow: KDU, 2007)
47. Siscoe G L, Chen C-K *J. Geophys. Res.* **80** 4675 (1975)
48. Saito T, Sakurai T, Yumoto K *Planet. Space Sci.* **26** 413 (1978)
49. Uffen R J *Nature* **198** 143 (1963)
50. Sagan C *Nature* **206** 448 (1965)
51. Kirkby J *Surv. Geophys.* **28** 333 (2007)
52. Kirkby M J et al. *Hydrol. Earth Syst. Sci.* **15** 3741 (2011)
53. Sinnhuber B-M et al. *Geophys. Res. Lett.* **30** 1580 (2003)
54. Melott A L et al. *Geophys. Res. Lett.* **32** L14808 (2005)
55. Vogt J et al. *J. Geophys. Res.* **112** 6216 (2007)
56. Winkler H et al. *J. Geophys. Res.* **113** 2302 (2008)
57. Svensmark H, Friis-Christensen E *J. Atmos. Solar Terr. Phys.* **59** 1225 (1997)
58. Lemair J F, Singer S F, in *Dynamics of the Earth's Radiation Belts and Inner Magnetosphere* (Geophysical Monograph, Vol. 199, Eds D Summers et al.) (Washington, DC: American Geophysical Union, 2012) p. 355
59. Doake C S M *Nature* **267** 415 (1977)
60. Simpson J F *Geol. Soc. Am. Bull.* **77** 197 (1966)
61. Doake C S M *Earth Planet. Sci. Lett.* **38** 313 (1978)
62. Opdyke N D *Int. J. Bioclimat. Biometeorol.* **3** 253 (1959)
63. Watkins N D, Goodell H G *Science* **156** 1083 (1967)
64. Black D I *Earth Planet. Sci. Lett.* **3** 225 (1967)
65. Harrison C G A, Somayajulu B L K *Nature* **212** 1193 (1966)
66. Zarrouk N, Bennaceur R *Int. J. Astrobiol.* **8** (3) 169 (2009)
67. Ponert J, Príhoda P, in *Bioastronomy 2007: Molecules, Microbes and Extraterrestrial Life, Proc. of a Workshop, 16 – 20 July 2007, San Juan, Puerto Rico* (ASP Conf. Ser., Vol. 420, Eds K J Meech et al.) (San Francisco: Astronomical Society of the Pacific, 2009) p. 259